APPLIED AND ENVIRONMENTAL MICROBIOLOGY, Oct. 1986, p. 866–874
0099-2240/86/100866-09$02.00/0
Copyright © 1986, American Society for Microbiology
Vol. 52, No. 4

Method for Assessing Heterogeneity in Turnover Rates within Microbial Communities†

EDWARD A. LAWS,[1,2]* DAVID JONES,[1] AND DAVID M. KARL[1]

Department of Oceanography, University of Hawaii, Honolulu, Hawaii, 96822,[1] and Hawaii Institute of Marine Biology, Coconut Island, Kaneohe, Hawaii, 96744[2]

Received 11 February 1986/Accepted 25 July 1986

A method is presented for determining both the average turnover rate and the standard deviation of the average turnover rate of the adenine nucleotide (AN) pool within a population of microorganisms. The method requires the calculation of the initial slope and curvature of a plot of AN specific activity versus time following the introduction of [^{3}H]adenine. An analysis of noise-corrupted data indicated that the method is capable of detecting a lack of uniformity in the turnover rate when the coefficient of variation of the turnover rate exceeds 39%. An analysis of field data revealed a significant lack of uniformity in the turnover rates of microbial communities in a marine sediment sample and freshwater pond but no significant nonuniformity in the turnover rates of microbial communities in a seawater sample and in a second freshwater pond. Although the method has been applied only to the analysis of AN turnover rates, it is applicable to any intracellular pool for which a suitable radioactive precursor exists.

In recent years, much attention in aquatic microbial ecology has been focused on the measurement of growth rates (4, 6, 18, 24; D. M. Karl and C. D. Winn, Limnol. Oceanogr., in press). The experimental methods that have been developed rely upon both autecological and synecological approaches. The autecological approaches include single-cell isolation techniques and the direct measurement of nuclear division (22, 26–28). These methods yield average values for the growth rate (μ) of individual species of microorganisms within a mixed-species assemblage (20, 21, 25). The synecological approaches include the measurement of the rate of nucleic acid synthesis (5, 13), the frequency of dividing cells (7), the estimation of chlorophyll *a* labeling (20), and the simultaneous determination of total biomass and carbon production. All of these community estimates of μ, in fact, yield some average value for all of the organisms in the sampled population. Although heterogeneity in metabolic activity and growth rate within microbial populations is generally acknowledged or presumed to occur, there remain few alternatives to qualitative techniques for assessing such variability. It would be desirable to have quantitative data which are directly relevant to currently used measurements of growth rate. Adenine nucleotides (ATP, ADP, and AMP) are present in all living cells and have well-established roles in cellular energetics, biosynthesis, and metabolic regulation. The adenine nucleotide (AN) pool turnover time is a direct measure of the rate at which these compounds are utilized by the cell for net nucleic acid synthesis. In theory, there should be a direct proportionality between growth rate and AN pool turnover rate (2), and the AN pool turnover rate can be measured for field-collected samples (14, 15). We have devised a novel method of data analysis which provides a quantitative measure of the variability in AN pool turnover rates, and in this paper we show that the same general approach is also applicable to the analysis of variability in turnover rates of other intracellular pools. The problem we have addressed has an analog in chemical engineering, in which the characteristics of the residence time distribution function of molecules in a reactor has been a subject of experimental investigation by techniques similar to those used here (23).

THEORY

The definitions of symbols used in the following derivations are given in Table 1. The distribution of AN pool turnover rates is assumed to be described by a function f (R) such that in the limit as dR approaches zero, the fraction of the AN pool with turnover rates between R and $R + dR$ is f(R)dR. Since the turnover rate of the AN molecules must lie somewhere between zero and infinity, it follows that

$$\int_0^\infty \mathrm{f}(R)dR = 1$$

If a radioactive precursor is introduced at $t = 0$ and if the specific radioactivity of the precursor remains constant during the incubation period, then the specific radioactivity $A(R,t)$ of the AN pools with turnover rates between R and $R + dR$ will be given by the expression $A(R,t) = A_p(1 - e^{-Rt})$, where A_p is the specific activity in the limit as t approaches infinity. The average specific activity, $A_{av}(t)$, of the AN pool as a function of time is given by the expression

$$A_{av}(t) = \int_0^\infty \mathrm{f}(R)A(R,t)dR = A_p \int_0^\infty \mathrm{f}(R)(1 - \mathrm{e}^{-Rt})dR \quad (1)$$

The first and second derivatives of $A_{av}(t)$ with respect to time are as follows:

$$dA_{av}(t)/dt = A_{av'} = A_p \int_0^\infty \mathrm{f}(R)(Re^{-Rt}) \quad (2)$$

$$d^2A_{av}(t)/dt^2 = A_{av''} = -A_p \int_0^\infty \mathrm{f}(R)R^2e^{-Rt} \quad (3)$$

When $t = 0$, it is obvious from equations 2 and 3 that

* Corresponding author.

† Hawaii Institute of Marine Biology contribution no. 723.

Downloaded from aem.asm.org at Univ of Hawaii at Manoa on March 30, 2010

TABLE 1. Definitions of symbols

Symbol	Definition
$A(R,t)$	Specific radioactivity of AN at time t with turnover rates between R and $R + dR$
AN	Adenine nucleotides
A_p	Asymptotic specific radioactivity of the AN pool as $t \rightarrow \infty$
$A_{av}(t)$	Average specific radioactivity of the AN pool at time t
$A_{av'}$	First derivative of A_{av} with respect to time
$(A_{av'})_0$	Value of $A_{av'}$ at $t = 0$
$A_{av''}$	Second derivative of A_{av} with respect to time
$(A_{av''})_0$	Value of $A_{av''}$ at $t = 0$
CV	Coefficient of variation of R
dR	Infinitesmally small increment in R
$f(R)$	Normalized distribution function of R
K	Exponential decay constant for least-squares fit (Fig. 1)
M	Intercept of least-squares fit to data (Fig. 1) provides estimate of $(R^2)_{av}/(R_{av})^2$
R	Turnover rate with possible values between 0 and ∞
R_0	Invariant turnover rate
R_{av}	Average value of R for all AN
$(R^2)_{av}$	Average value of R^2 for all AN
SD	Standard deviation of R
Δt	Finite increment in time
V	Variance of R

$$dA_{av}(t)/dt = (A_{av'})_0 = A_p \int_0^\infty f(R)RdR = A_p(R_{av}) \quad (4)$$

$$d^2A_{av}(t)/dt^2 = (A_{av''})_0 = -A_p \int_0^\infty f(R)R^2dR$$

$$= -A_p(R^2)_{av} \quad (5)$$

Thus, R_{av}, the average value of R, can be determined by simply dividing the slope of the function $A_{av}(t)$ at $t = 0$ by A_p, while $(R^2)_{av}$, the average value of R^2, can be determined by dividing the curvature of $A_{av}(t)$ (i.e., second derivative) at $t = 0$ by $-A_p$. Given R_{av} and $(R^2)_{av}$, the variance of R can be calculated from the expression

$$V = \int_0^\infty f(R)(R - R_{av})^2dR = (R^2)_{av} - (R_{av})^2 \quad (6)$$

Given this information, it is straightforward to calculate the standard deviation, $SD = V^{1/2}$, and the coefficient of variation, $CV = SD/R_{av}$, of the distribution of turnover rates. Note that $CV = [(R^2)_{av}/(R_{av})^2 - 1]^{1/2}$.

In practice, $A_{av}(t)$ is measured at discrete points in time, and to calculate R_{av} and $(R^2)_{av}$ from equations 4 and 5 it is necessary to obtain an accurate estimate of A_p and to estimate the first and second derivatives of A_{av} at the origin by finite-difference approximations. It is theoretically possible to determine both upper and lower bounds to A_p. The upper bound is the value of the specific activity of the exogenous precursor pool corrected for isotope discrimination. This value will be an overestimate of the true value of A_p to the extent that de novo synthesis pathways and intracellular pools effectively dilute the precursor specific activity (17). A lower bound may be obtained in either of two ways. First, the value of $A_{av}(t)$ for any finite value of t is obviously less than A_p, and the largest value of $A_{av}(t)$ is therefore a lower bound to A_p to within the precision with which $A_{av}(t)$ can be measured. Second, we have found that, in practice, the value of A_p estimated from a nonlinear least-squares fit of the function $A_p(1 - e^{-Rt})$ to a time series of $A_{av}(t)$ values will systematically underestimate the true A_p unless all the AN are in fact turning over at the same rate. This result follows from the fact that when there is a distribution of R values, a fit of the function $A_p(1 - e^{-Rt})$ to the data invariably leads to an underestimation of $A_{av}(t)$ for small values of t, an overestimation of $A_{av}(t)$ for intermediate values of t, and an underestimation of $A_{av}(t)$ for large values of t. When there is little difference between the upper bound to A_p and the larger of the two lower bounds, one can obviously estimate A_p with a high degree of confidence. One good check on the accuracy of the A_p estimate comes from the fact that when $(A_{av'})_0$ and $(A_{av''})_0$ are approximated by finite differences, the expression $-A_p(A_{av'})_0/(A_{av''})_0^2$ must approach unity in the limit as Δt approaches infinity and must be greater than or equal to unity for all finite values of Δt (see below). Since the value of this expression is directly proportional to the value assigned to A_p, the behavior of the expression as a function of Δt provides a good indication of the accuracy of the A_p estimate. The first and second derivatives of $A_{av}(t)$ at $t = 0$ are approximated by using one-sided finite difference equations accurate to order Δt, where Δt is the time interval between data points (9). These finite difference approximations are as follows:

$$dA_{av}(t)/dt|_{t=0} \approx A_{av}(\Delta t)/\Delta t \quad (7)$$

$$d^2A_{av}(t)/dt^2|_{t=0} \approx [A_{av}(2\Delta t) - 2A_{av}(\Delta t)]/(\Delta t)^2 \quad (8)$$

Equations 7 and 8 make use of the fact that $A_{av}(0) = 0$. Although it is possible to use higher-order finite difference approximations to estimate the derivatives of $A_{av}(t)$, these higher-order approximations become increasingly sensitive to analytical noise in the data. Even equations 7 and 8 become unacceptably sensitive to analytical noise as Δt becomes small, and, in practice, a compromise must usually be struck between choosing small values of Δt to minimize the truncation error in the finite difference approximations and choosing large values of Δt to minimize the error created by analytical noise.

MATERIALS AND METHODS

Sample collection and incubation. Water samples were collected from two freshwater ponds (Krauss Pond and Quarry Pond) located on the University of Hawaii campus and from a nearshore (ca. 1 km offshore) station located off the leeward coast of Oahu. All samples were collected in acid-washed polycarbonate bottles, prefiltered on-site through a 90-μm-pore-size Nitex mesh (Tetko, Inc.) and returned to the laboratory, where the experiments were performed within 1 h of sample collection. [^{3}H]adenine (15 Ci mmol^{-1}; New England Nuclear Corp.) was added to each water sample to yield a final concentration of 0.1 μCi of [^{3}H]adenine ml^{-1}. All incubations were performed at approximate in situ temperature (24°C) during daylight hours in full sunlight. We also analyzed a sediment population collected from Kahana Bay, Oahu. A sediment core was collected by hand, and the sediment-water interface layer was immediately removed by aspiration as previously described (19). This sample was placed in an acid-washed polycarbonate bottle and was transported to the laboratory,

Downloaded from aem.asm.org at Univ of Hawaii at Manoa on March 30, 2010

TABLE 2. Twelve hypothetical distribution functions for f(R), corresponding exact expressions for $A_{av}(t)/A_p$ and $(R^2)_{av}/(R_{av})^2$, and approximate values (M) for $(R^2)_{av}/(R_{av})^2$ determined from least-squares fits to data in Fig. 3[a]

Example	f(R)	$A_{av}(t)/A_p$	$(R^2)_{av}/(R_{av})^2$ (exact)	M
1	$\delta(R - R_0)$	$1 - e^{-R_0t}$	1	1
2	$(R/R_0^2)e^{-R/R_0}$	$1 - 1/(1 + R_0t)^2$	1.50	1.43
3	$0.5(R^2/R_0^3)e^{-R/R0}$	$1 - 1/(1 + R_0t)^3$	4/3 (ca. 1.33)	1.29
4	$0.2\delta(R - R_0) + 0.8\delta(R - 2R_0)$	$1 - 0.2e^{-R_0t} - 0.8e^{-2R_0t}$	85/81 (ca. 1.05)	1.05
5	$0.5[\delta(R - R_0) + \delta(R - 2R_0)]$	$1 - 0.5(e^{-R_0t} + e^{-2R_0t})$	10/9 (ca. 1.11)	1.12
6	$0.8\delta(R - R_0) + 0.2\delta(R - 2R_0)$	$1 - 0.8e^{-R_0t} - 0.2e^{-2R_0t}$	10/9 (ca. 1.11)	1.11
7	$0.2\delta(R - R_0) + 0.8\delta(R - 4R_0)$	$1 - 0.2e^{-R_0t} - 0.8e^{-4R_0t}$	325/289 (ca. 1.12)	1.13
8	$0.5[\delta(R - R_0) + \delta(R - 4R_0)]$	$1 - 0.5(e^{-R_0t} + e^{-4R_0t})$	34/25 (ca. 1.36)	1.38
9	$0.8\delta(R - R_0) + 0.2\delta(R - 4R_0)$	$1 - 0.8e^{-R_0t} - 0.2e^{-4R_0t}$	25/16 (ca. 1.56)	1.57
10	$0.2\delta(R - R_0) + 0.8\delta(R - 8R_0)$	$1 - 0.2e^{-R_0t} - 0.8e^{-8R_0t}$	1,285/1,089 (ca. 1.18)	1.20
11	$0.5[\delta(R - R_0) + \delta(R - 8R_0)]$	$1 - 0.5(e^{-R_0t} + e^{-8R_0t})$	130/81(ca. 1.60)	1.65
12	$0.8\delta(R - R_0) + 0.2\delta(R - 8R_0)$	$1 - 0.8e^{-R_0t} - 0.2e^{-8R_0t}$	85/36 (ca. 2.36)	2.38

[a] $\delta(a - x)$ is defined by the equation $g(a) = \int_{-\infty}^{\infty} \delta(a - x)g(x)dx$ for any function g.

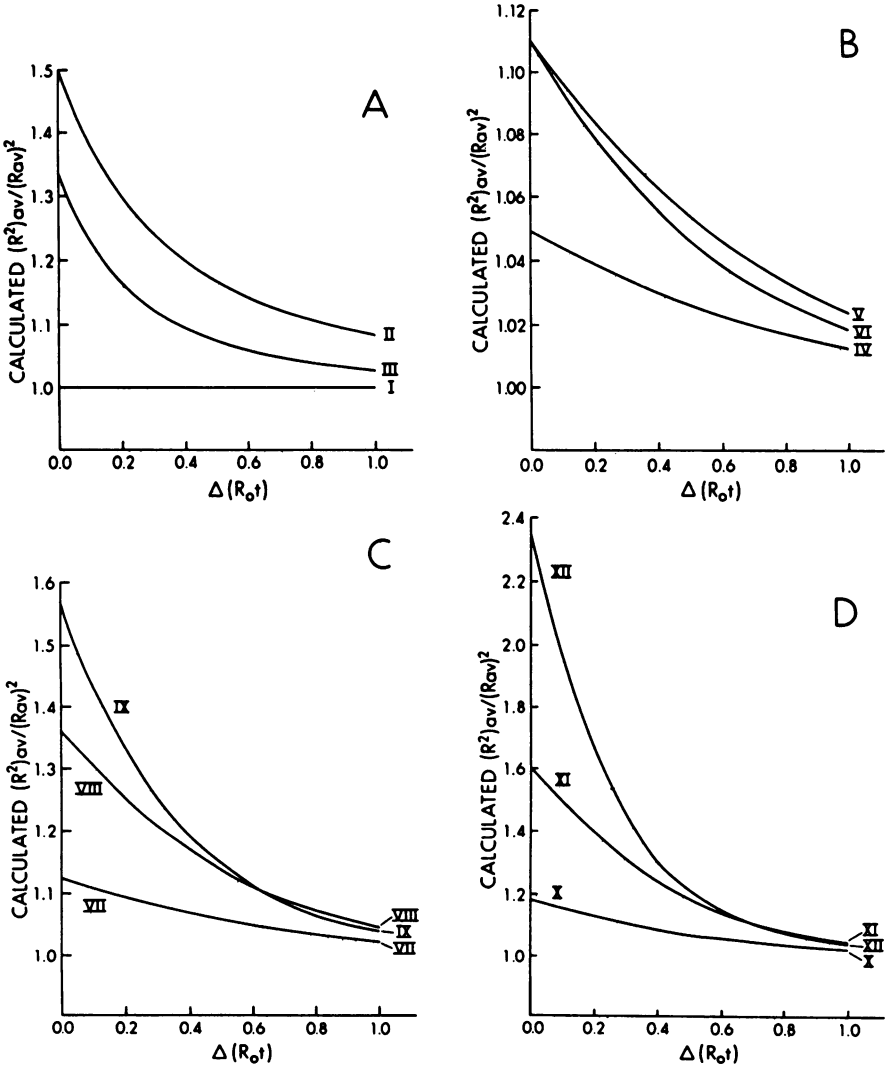


FIG. 1. Effect of varying $\Delta(R_0t)$ on the value of $(R^2)_{av}/(R_{av})^2$ calculated from equations 4, 5, 7, and 8 for the 12 hypothetical functions in Table 1.

Downloaded from aem.asm.org at Univ of Hawaii at Manoa on March 30, 2010

TABLE 3. Analysis of effect of analytical noise on calculated values of M for examples in Table 2[a]

Example	$(R^2)_{av}/(R_{av})^2$ (exact)	Mean $M \pm$ SD	% of cases in which $M > 1.0$
1	1.00	1.07 ± 1.22	55
2	1.50	1.52 ± 0.40	100
3	1.33	1.38 ± 0.35	96
4	1.05	1.12 ± 0.62	69
5	1.11	1.22 ± 0.62	78
6	1.11	1.22 ± 0.85	71
7	1.12	1.20 ± 0.25	91
8	1.36	1.46 ± 0.35	99
9	1.56	1.73 ± 0.61	99
10	1.18	1.23 ± 0.19	97
11	1.60	1.67 ± 0.23	100
12	2.36	2.50 ± 0.57	100

[a] In each case, 500 noise-corrupted data sets were assumed to have been measured in triplicate, with the standard deviation of a single measurement being 5% of the true value at that point. For other details, see text.

where the time course incubation experiment was performed. [^{3}H]adenine was added to the sediment slurry to yield a final concentration of 0.3 μCi ml^{-1}, and the samples were incubated at 24°C in room light on a slow-speed gyratory shaker table (20 to 25 rpm).

ATP pool extraction and measurement of specific activity. For each water sample, we performed a time course extraction of cellular ATP at predetermined intervals. For water samples, cellular ATP was concentrated onto a Whatman glass fiber filter (GF/F) and extracted in boiling phosphate buffer (60 mM, pH 7.4). ATP and [^{3}H]ATP were purified and measured as previously described (17). The specific radioactivity of the sediment samples was measured at each time point by injection of a 0.5-ml portion of the sediment slurry into 5 ml of boiling phosphate buffer followed by sample concentration and purification as described by Craven and Karl (3).

RESULTS

Theoretical results. (i) Truncation error. As a first test of the proposed method, we examined the effect of truncation error on the calculated values of $(R^2)_{av}/(R_{av})^2$ from artificial data sets generated from hypothetical microbial communities with various assumed distributions of AN pool turnover rates. The 12 hypothetical distribution functions which we examined are listed in Table 2. Three of the distribution functions were unimodal, and one of these (example 1) corresponded to a community with a single turnover rate. The remaining distribution functions were bimodal and were distinguished by varying the relative biomasses of the component populations and the difference in their turnover rates. The exact values of $(R^2)_{av}/(R_{av})^2$ for each distribution function are listed in Table 2, and the calculated values of $(R^2)av/(R_{av})^2$ as a function of the dimensionless parameter $\Delta(R_0t)$ are shown for each case in Fig. 1.

Several features of the results in Fig. 1 are noteworthy. First, it is apparent from Fig. 1A that the truncation error in the calculation of $(R^2)_{av}/(R_{av})^2$ from equations 7 and 8 is zero for a population having a single turnover rate. This result is perhaps surprising, because the truncation errors in the calculation of $(A_{av}')_0$ and $(A_{av}')_0$ are nonzero. However, it can be shown mathematically that these errors exactly cancel when the ratio $(A_{av}')_0/(A_{av}')_0^2$ is calculated from equations 7 and 8 to estimate $(A_{av}')_0$ and $(A_{av}')_0$ and if $A_{av}(t) = A_p(1 - e^{-R_0t})$. This result is quite appealing, since one is assured that the finite-difference scheme proposed here for approximating $(A_{av}')_0$ and $(A_{av}')_0$ will lead to accurate and unbiased estimates of $(R^2)_{av}/(R_{av})^2$ regardless of the choice of Δt whenever the turnover rate is the same for all organisms in the population.

A second characteristic of the results in Fig. 1 is that all the calculated values of $(R^2)_{av}/(R_{av})^2$ approach unity in the limit as $\Delta(R_0t)$ approaches infinity. This result can be explained from an examination of equation 1. As Δt becomes large, the value of $[1 - \exp(-Rt)]$ becomes essentially constant and equal to unity for all but the smallest values of R. Therefore, the range of values of R which effectively contribute to the time dependence of $A_{av}(t)$ becomes progressively smaller as t becomes large. Consequently, in the limit of large t, the first and second derivatives of $A_{av}(t)$ cannot be distinguished from the first and second derivatives of a function describing a population with only a single turnover rate. This conclusion will be true for any $f(R)$.

A final point about Fig. 1 is that in all cases but example 1, the truncation error is positively correlated with $\Delta(R_0t)$. Furthermore, all plots of the calculated $(R^2)_{av}/(R_{av})^2$ ratios exhibit positive curvature. Since, in practice, a time series of $A_{av}(t)$ is anticipated, one method for estimating the true $(R^2)_{av}/(R_{av})^2$ would be the calculation of this ratio for various values of Δt and extrapolation of the calculated values back to $\Delta t = 0$. To test the feasibility of this approach, we attempted to fit each of the data sets in Fig. 1 to a function of the form $1 + (M - 1)\exp[-K\Delta(R_0t)]$. This function was chosen because it satisfies the constraint of extrapolating to unity as $\Delta(R_0t)$ becomes large and because it displays the positive curvature characteristic of all the curves in Fig. 1. M and K were chosen to minimize the sum of the squares of the derivations of the empirical function from the actual data points, and the value of the function at $\Delta(R_0t) = 0$ (i.e., M) was compared with the true value of $(R^2)_{av}/(R_{av})^2$. In performing the least-squares analysis, a total of 9 or 10 equally spaced datum points were chosen over the time interval corresponding to $A_{av}(t)/A_p = 0.2$ to 0.8. Smaller values of $\Delta(R_0t)$ were not used because error analysis revealed that the finite-difference approximation to $(A_{av}')_0$ (equation 8) becomes too sensitive to analytical noise when $A_{av}(t)/A_p \leq 0.2$ (see below). Comparisons of the exact values of $(R^2)_{av}/(R_{av})^2$ with the values of M calculated from the least-squares fits are shown in Table 2. The agreement between the exact and approximate values of $(R^2)_{av}/(R_{av})^2$ is excellent, the largest discrepancy being less than 5% of the exact value. The use of time series data and this curve-fitting procedure therefore appears to be useful for dealing with the problem of truncation error.

(ii) Analytical noise. To study the effect of analytical noise on the calculated values of $(R^2)_{av}/(R_{av})^2$, we generated noise-corrupted data by using the assumption that the standard deviation of an individual AN pool specific activity measurement was 5% of the measured value (see Field Results). The specific-activity measurements at each time point were assumed to have been made in triplicate. Noise-corrupted values of $A_{av}(t)/A_p$ were generated by choosing random numbers which followed a normal distribution with a mean equal to the correct value of $A_{av}(t)/A_p$ (from the equations in Table 2) and a standard deviation equal to 5% of this value. For each of the 12 examples in Table 2, a total of 500 noise-corrupted data sets were analyzed. Each data set contained 10 datum points chosen at equally spaced values of R_0t, with the first value of R_0t being chosen to correspond to $A_{av}(t)/A_p = 0.2$ to 0.3 for the first datum point in the function without noise corruption. For smaller values of R_0t,

Downloaded from aem.asm.org at Univ of Hawaii at Manoa on March 30, 2010

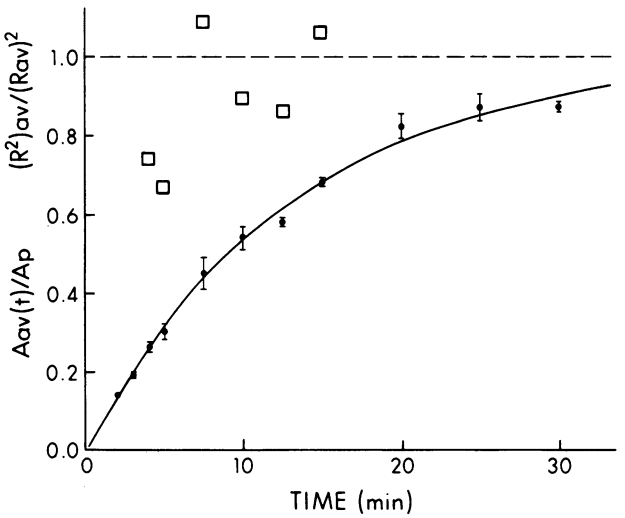


FIG. 2. Plot of $A_{av}(t)/A_p$ (●) and calculated values of $(R^2)_{av}/(R_{av})^2$ (□) for Quarry Pond data. The smooth curve is a fit of $1 - \exp(-Rt)$ to $A_{av}(t)/A_p$ data. Error bars are standard errors of the mean.

the value of $(A_{av})_0$ calculated from equation 8 was found to be unacceptably sensitive to analytical noise. A nonlinear least-squares routine was used to fit the function $1 + (M - 1)\exp(-Kt)$ to each noise-corrupted data set, and the mean

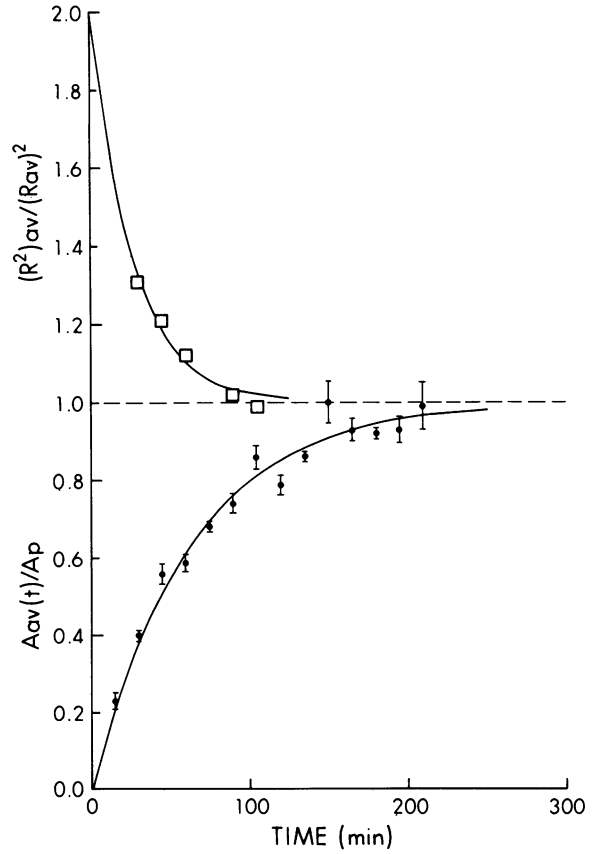


FIG. 3. Plot similar to Fig. 2 for Krauss Pond data. The smooth curve in the upper figure is a least squares fit of $1 + (M - 1)\exp(-Kt)$ to $(R^2)_{av}/(R_{av})^2$ data.

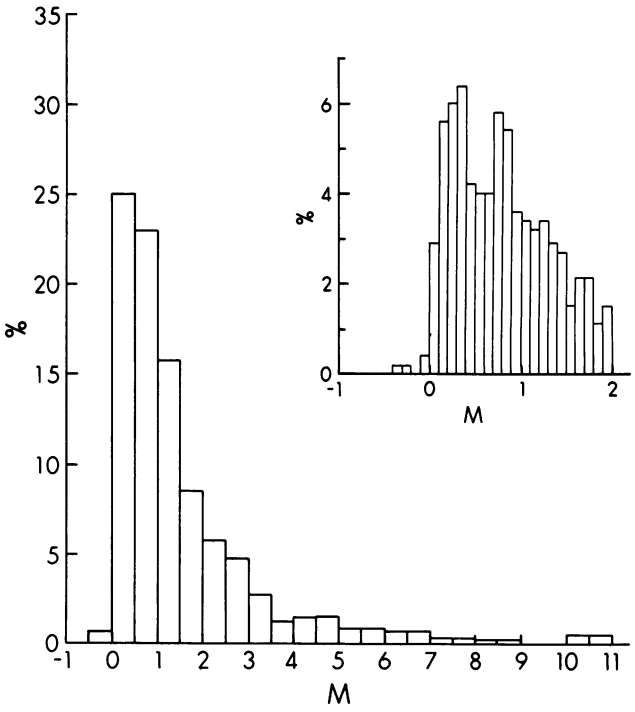


FIG. 4. Histogram of M values generated from noise-corrupted data sets for Krauss Pond data.

and standard deviation of the calculated values of M were determined. The number of times the calculated value of M was less than unity was also recorded.

The results of this exercise (Table 3) are noteworthy in two respects. First, the averages of the calculated values of M are in all cases close to the true value of $(R^2)_{av}/(R_{av})^2$ and in most cases differ by no more than 0.1 (maximum deviation, 0.17). In all cases, the mean values of M are slight overestimates of the true value of $(R^2)_{av}/(R_{av})^2$. An analysis of the distribution of calculated values of M revealed that, although the errors in the measured values of $A_{av}(t)/A_p$ were assumed to follow a normal distribution, the resulting errors in M are not normally distributed. The distribution of calculated values of M is skewed somewhat to the right, and this fact largely accounts for the tendency of the mean value to overestimate $(R^2)_{av}/(R_{av})^2$. Since the distribution of M values does not follow a normal distribution, the standard deviation of M, while a meaningful statistic in itself, cannot be used to determine the statistical significance of M by standard methods.

Second, since $(R^2)_{av} - (R_{av})^2 = [(R - R_{av})^2]_{av} \geq 0$, it is obvious that $(R^2)_{av}/(R_{av})^2 \geq 1$, and in fact will equal unity only in the limiting case in which all the AN in the population is turning over at the same rate. In the analysis of field data, an appropriate null hypothesis would therefore be that all the AN is turning over at the same rate [i.e., $(R^2)_{av}/(R_{av})^2 = 1$], and the test for rejection of this hypothesis would be one-sided, since $(R^2)_{av}/(R_{av})^2 < 1$ is impossible. A critical question is therefore how often analytical noise causes the calculated value of M to be less than unity. The analysis in Table 3 indicates that the assumed level of analytical noise causes the calculated value of M to be less than unity more than 5% of the time when the true value of $(R^2)_{av}/(R_{av})^2 <$ ca. 1.15. Thus, given the assumed level of analytical noise, one would expect to be able to reject the null hypothesis that all

Downloaded from aem.asm.org at Univ of Hawaii at Manoa on March 30, 2010

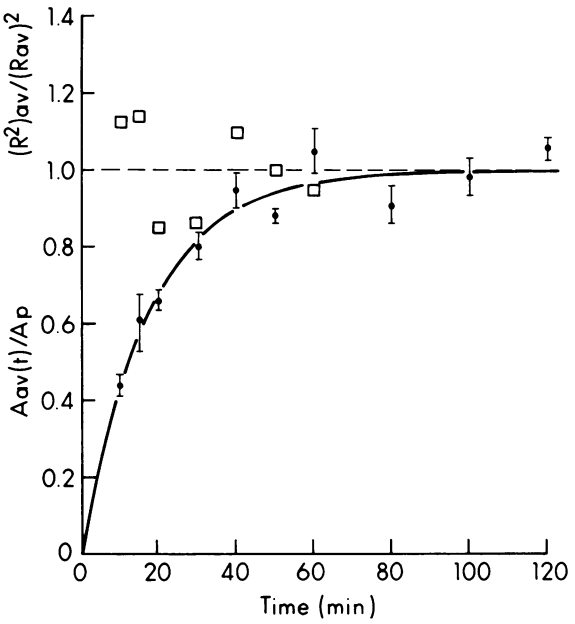


FIG. 5. Plot similar to Fig. 2 for leeward Oahu data.

the ATP molecules are turning over at the same rate with a confidence of at least 95% whenever the true value of $(R^2)_{av}/(R_{av})^2 > 1.15$, or in other words, when the CV = $(1.15 - 1.00)^{1/2} = 0.39$. Given this conclusion, we now turn to an analysis of data collected from natural populations.

Field Results. Figures 2 and 3 show results obtained from two freshwater ecosystems, Quarry Pond and Krauss Pond, respectively. In both cases, a function of the form $A_p[1 - \exp(-Rt)]$ gave an excellent fit to the experimental $A_{av}(t)$ data, a fact which initially suggested that there was little heterogeneity in the AN pool turnover rates within either pond. For Quarry Pond (Fig. 2), the specific activities measured at the first three time points were less than 20% of the asymptotic value, and therefore only the last nine values of $A_{av}(t)/A_p$ were used in the estimation of $(R^2)_{av}/(R_{av})^2$. These data included six pairs for which the sampling time differed by a factor of 2, and the values of $(R^2)_{av}/(R_{av})^2$ calculated from equations 4, 5, 7, and 8 at these six time points are shown in Fig. 2. There is no significant correlation between these calculated values of $(R^2)_{av}/(R_{av})^2$ and time ($r = 0.62$; $P > 0.10$), and the average of the six values (0.89 ± 0.075) is not significantly different from unity (t-test, $P > 0.20$). Both these results are consistent with the assumption that all AN pools in the population were turning over at the same rate.

For Krauss Pond (Fig. 3), the specific activities measured at the first time point and at 150 min were excluded from the calculations of $(R^2)_{av}/(R_{av})^2$. In the former case, the standard deviation of the triplicate measurements was too large (20% of the mean value), and in the latter case the datum point lies well above the smooth-curve fit to the data. The standard deviations of the remaining 12 datum points averaged 6% of the corresponding mean values, and the datum points contain a total of five pairs for which the sampling time differed by a factor of 2. The values of $(R^2)_{av}/(R_{av})^2$ calculated from these five pairs are shown in Fig. 3. These five values are highly correlated with time ($r = -0.98$, $P < 0.01$), and a fit of the function $1 + (M - 1)\exp(-Kt)$ to the data yielded $M = 2.0$. A total of 520 noise-corrupted data sets were generated by using the standard deviation of each set of triplicate measurements to corrupt the data, and analysis of these data sets yielded only six cases out of 520 (1.15%) in which $M \leq 1$. Thus, in this case, one can reject the null hypothesis that $(R^2)_{av}/(R_{av})^2 = 1$ with a high degree of confidence. A frequency distribution of the calculated values of M for the 520 noise-corrupted data sets is shown in Fig. 4. The skewed nature of the distribution function is clearly apparent from these data. On the basis of this distribution function, the 95% confidence interval for $(R^2)_{av}/(R_{av})^2$ was calculated to be 1.06 to 17, which corresponds to a confidence interval of 0.24 to 4 for the CV. The value of the CV calculated from the fit to the uncorrupted data, 1.0, is therefore almost exactly the geometric mean of these two confidence limits.

Figures 5 and 6 show results obtained from two marine environments, a nearshore water sample from the leeward side of the island of Oahu and a sediment sample from Kahana Bay on the windward side of Oahu, respectively. Both data sets are reasonably well described by a function of the form $A_p[1 - \exp(-Rt)]$, although for the sediment data there is a tendency for the experimental data to exceed the least-squares curve for small values of t and to lie below the fitted curve for large values of t. For the results in Fig. 5, all values of $A_{av}(t)/A_p$ exceeded 0.2, and no datum points were excluded from the analysis. The calculated values of $(R^2)_{av}/(R_{av})^2$ showed no significant correlation with time ($r = -0.34$), and the mean value of the seven values (1.00 ± 0.12) was not significantly different from unity (t test, $P > 0.5$). As was the case for the Quarry Pond analysis (Fig. 2), both results are consistent with the assumption that the AN pools of all microorganisms in the population were turning over at the same rate.

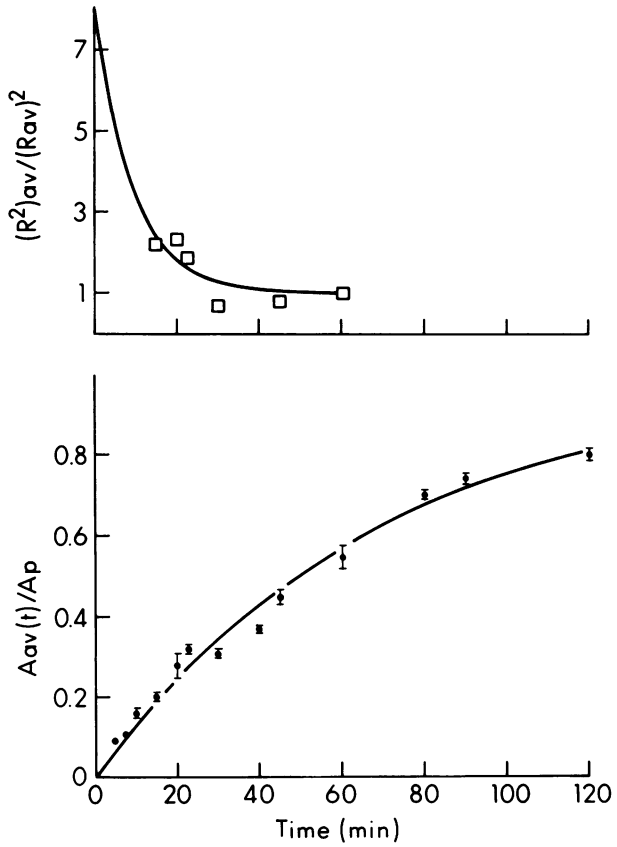


FIG. 6. Plot similar to Fig. 3 for Kahana Bay sediment data.

Downloaded from aem.asm.org at Univ of Hawaii at Manoa on March 30, 2010

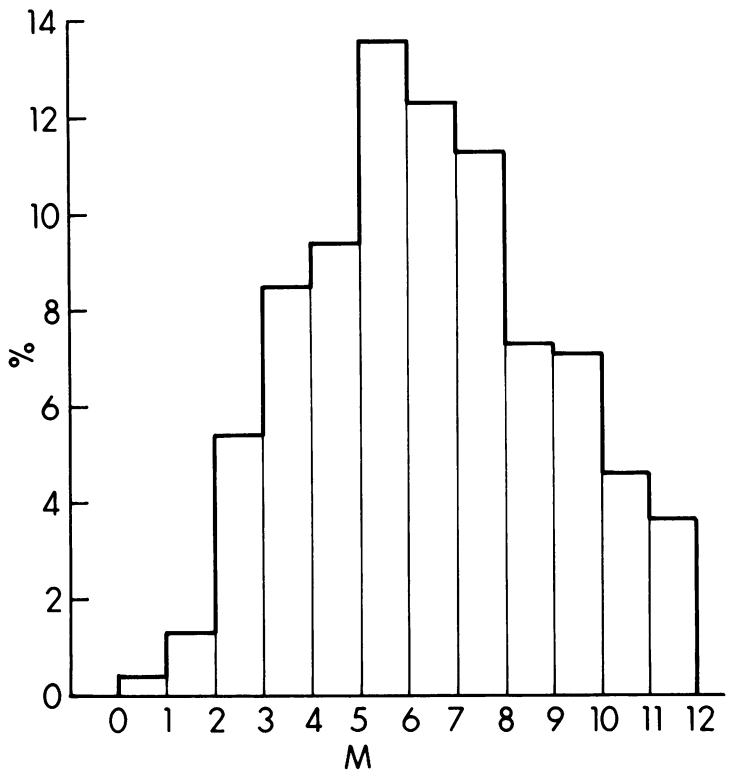


FIG. 7. Histogram similar to Fig. 4 for Kahana Bay noise-corrupted data.

For the Kahana Bay sediment data, the specific activities measured at times less than 15 min were less than 20% of the asymptotic value and were therefore excluded from the analysis. When values of $(R^2)_{av}/(R_{av})^2$ were estimated by using the remaining datum point pairs, the value calculated from the specific activities at 40 and 80 min was found to be unrealistically low (0.34) and was therefore excluded from the analysis. The remaining six values of $(R^2)_{av}/(R_{av})^2$ are shown in Fig. 6. A least-squares fit of the function $1 + (M - 1)\exp(-Kt)$ to these six datum points yielded $M = 8.0$. As for the Krauss Pond analysis, a total of 520 noise-corrupted data sets were generated by using the standard deviation of each set of triplicate measurements to corrupt the data. In this case, the standard deviations averaged 7% of the corresponding mean values. This analysis did not produce a single case in which $M \leq 1$, and one can therefore reject the null hypothesis that $(R^2)_{av}/R_{av})^2 = 1$ with a high degree of confidence. Examination of the frequency distribution of the calculated values of M (Fig. 7) indicated the 95% confidence interval for $(R^2)_{av}/(R_{av})^2$ to be 3.2 to 26, which corresponds to a confidence interval of 1.5 to 5.0 for the CV. The value of the CV calculated from the fit to the uncorrupted data, 2.6, is therefore again almost exactly the geometric mean of these two confidence limits.

DISCUSSION

Microbial communities in nature are expected to exhibit a certain degree of heterogeneity in their morphological, physiological, and genetic characteristics (1). This diversity among the individuals of a given microbial assemblage is typically measured by assessing the species richness by microscopic examination (10), isolation and taxonomic characterization (8, 11), or rRNA sequencing methods (25). In this paper, we present a method for assessing the diversity of metabolic rates among individuals of a given population or community. While the potential maximum growth rate of a selected individual is expected to be under genetic control, the in situ metabolic rate, or variability thereof, is expected to be under environmental control and cannot be predicted from species diversity indices alone. Consequently, there is no a priori reason to expect species diversity and the degree of in situ metabolic rate homogeneity to covary in natural microbial communities. The method described herein is based on the uptake of [^{3}H]adenine. As discussed previously (12, 16), this method is capable of measuring the growth rates of metabolically active bacteria and unicellular algae. Nongrowing individuals are not expected to exhibit net assimilation of [^{3}H]adenine under in situ conditions. It should be emphasized however, that $^{32}PO_4^{3-}$ (or $^{33}PO_4^{3-}$) could also be used to measure total microbial community AN pool turnover (14, 15) and $^{14}CO_2$ has been used to determine phytoplankton carbon turnover rates (20). Consequently, our approach is not restricted to the use of [^{3}H]adenine. In two of the four data sets presented herein (Fig. 2 and 5), we found no evidence for heterogeneity among the in situ metabolic rates of the sampled populations. While these data might be interpreted as a logical result from a habitat which is dominated (in terms of biomass and production) by a single species, we believe that the ultimate cause of the uniform turnover rate measured for these communities is the result of environmental factors rather than low species diversity. Although we did not evaluate independently the species composition or distribution of biomass among eucaryotic algae, cyanobacteria, and heterotrophic bacteria in our samples, subsequent epifluo-

Downloaded from aem.asm.org at Univ of Hawaii at Manoa on March 30, 2010

rescence microscopy examination of samples collected from both habitats confirmed the presence of both autotrophs and heterotrophs. These results indicated that all growing microorganisms from the sampled population are metabolically equivalent despite the genetic potential for physiological heterogeneity. Similar ecological results have been obtained by measurement of the AN pool turnover rates of size fractionated samples from the Antarctic peninsula (Karl and Winn, in press).

The data in Fig. 3 and 6 indicate that sufficient heterogeneity in AN turnover rate is present in these samples that we must reject our null hypothesis that all species of microorganisms have identical AN turnover rates. Although this preliminary data base is too restrictive to draw any firm ecological conclusions, it is interesting that both Krauss Pond (Fig. 3) and the surface sediment (depth, 0 to 1 cm) collected from Kahana Bay are characterized by a very high level of habitat diversity. In Krauss Pond, the diversity is maintained by nonliving particulate matter derived in part from allochthonous sources, and in Kahana Bay, the sediments and microzones maintain the diversity of habitats. Future studies should be designed to evaluate the relationships among habitat variability, metabolic rate heterogeneity, total productivity, and taxonomic diversity.

While we have elected to use AN as the metric in our experimental protocol, the approach described herein is also directly applicable to the analysis of variability in the turnover rates of most intracellular metabolite pools. One important criterion which must be considered is the magnitude of the metabolite pool turnover time relative to the average growth rate of the microbial population under investigation. Some caution must be exercised when the pool turnover rate is comparable to the growth rate of the organisms in question. For the intracellular AN pool, the turnover rate is 30 to 50 times the growth rate (2), and it is therefore reasonable to assume that the population structure does not change significantly during the time required to generate a specific activity curve (ca. 10% of the doubling time). However, longer incubation times would be required for the isotopic equilibration of intracellular metabolite pools with slower turnover rates, and in such cases the distribution function f(R) may conceivably change. However, temporal variability in the distribution function can be taken into account by expressing f as a function both of R and t, i.e., f = f (R,t). In that case, equation 2 becomes

$$A_{av'} = A_p \int_0^\infty [f(R,t)\, Re^{-Rt} + f'(R,t)(1 - e^{-Rt})]dR \quad (9)$$

and equation 3 becomes

$$A_{av''} = A_p \int_0^\infty [-f(R,t)R^2e^{-Rt} + f''(R,t)\,(1 - e^{-Rt}) + 2f''(R,t)Re^{-Rt}]dR \quad (10)$$

At t = 0, equations 9 and 10 become

$$(A_{av'})_0 = A_p \int_0^\infty f(R,0)RdR = (A_p)(R_{av})_0 \quad (11)$$

$$(A_{av''})_0 = A_p \int_0^\infty [-f(R,0)R^2 + 2f''(R,0)R]dR = -A_p(R^2)_{av} + 2A_p(R_{av})_{0'} \quad (12)$$

Equation 11 is identical to equation 4, but equation 12 differs from equation 5 owing to the presence of the additional term $2A_p(R_{av})_{0'}$, where $(R_{av})_{0'}$ is the rate of change with respect to time of R_{av} at t = 0. It is straightforward to correct for the presence of this additional term, since $(R_{av})_{0'}$ can easily be estimated by performing two separate incubations offset in time by a time interval T. The initial slopes of plots of specific activity versus time for these two incubations will yield values of R_{av} at time zero and at time T, and $(R_{av})_0$ may then be estimated from the equation $(R_{av})_0 = [(R_{av})_T - (R_{av})_0]/T$. Thus, temporal variability in R_{av} should be considered when analyzing variability in turnover rates which are comparable to growth rates, but from a theoretical and experimental standpoint, the appropriate correction is straightforward.

An additional concern is the possibility that A_p varies among different members of the microbial community. Differences in A_p would reflect differences in the relative importance of salvage pathways and de novo synthesis in the production of AN. If such differences in the relative importance of salvage pathways and de novo synthesis are functions of the turnover rate R, then the derivations given here must be modified. In particular, A_p must be included in the integrand of equation 1, and the expressions for $(A_{av'})_0$ and $(A_{av''})_0$ become

$$(A_{av'})_0 = (A_pR)_{av} \quad (13)$$

$$(A_{av''})_0 = -(A_pR^2)_{av} \quad (14)$$

When there is only one value of R, this distinction is (of course) of no consequence. However, what are the implications when there is a distribution of R values? In that case, we note that the covariance (COV) of A_p with R^n is given by the equation

$$\text{COV} = \int_0^\infty f(R)[A_p(R) - (A_p)_{av}][R^n - (R^n)_{av}]dR = (A_pR^n)_{av} - (A_p)_{av}(R^n)_{av}$$

Hence the right-hand sides of equations 13 and 14 can be well approximated by $(A_pR)_{av} \approx (A_p)_{av}(R)_{av}$ and $-(A_pR^2)_{av} \approx -(A_p)_{av}(R^2)_{av}$, respectively, as long as the covariance of A_p with R and R^2 is small. We believe that this assumption is a good one, because we know of no reason why the relative importance of salvage pathways and de novo synthesis should covary with R or R^2. Hence even in the case in which A_p is not independent of R, the equations we have given should be useful for estimating $(R^2)_{av}/(R_{av})^2$ and for deciding whether this ratio deviates significantly from unity.

A final comment concerns the usefulness of the results obtained from the procedures outlined here. Although the mean and variance of a particular parameter are well-defined statistics, they must be used with caution in performing statistical tests when the underlying distribution factor is unknown. While our methods provide estimates of the mean and variance of AN turnover rates, these statistics by themselves give no indication of whether f(R) is well approximated by a normal distribution function or deviates significantly from normality. In fact, we have no way of telling whether f(R) is unimodal or polymodal, symmetric or asymmetric. Given these limitations, it seems inadvisable to use the mean and variance of R in any statistical tests (e.g., the t test) which assume a well-defined form of f(R).

Our attitude is that the principal utility in knowing the mean and variance of R will be in the interpretation of data

Downloaded from aem.asm.org at Univ of Hawaii at Manoa on March 30, 2010

concerning community growth and production rates obtained by other methods. For example, nucleic acid synthesis rates estimated from the uptake of tritiated adenine are calculated on the assumption that the specific activities of the intracellular AN pools are the same for all microorganisms within the population (13), and estimates of phytoplankton growth rates based on the incorporation of ^{14}C into chlorophyll *a* are similarly based on the assumption that specific activities of the chlorophyll *a* in all phytoplankton cells are the same (20). Violation of such assumptions as a result of nonuniformity in metabolic rates could lead to biased estimates of production and growth rates. The method we have outlined here should therefore prove useful in interpreting the results of such microbial production and growth rate measurements.

LITERATURE CITED

1. **Atlas, R. M.** 1984. Diversity of microbial communities. Adv. Microb. Ecol. **7**:1–47.
2. **Chapman, A. G., and D. E. Atkinson.** 1977. Adenine nucleotide concentration and turnover rates. Their correlation with biological activity in bacteria and yeast. Adv. Microb. Physiol. **15**:254–306.
3. **Craven, D. C., and D. M. Karl.** 1984. Microbial RNA and DNA synthesis in marine sediments. Mar. Biol. (Berlin) **83**:129–139.
4. **Ducklow, H. W., and S. M. Hill.** 1985. Tritiated thymidine incorporation and the growth of heterotrophic bacteria in warm core rings. Limnol. Oceanogr. **30**:260–272.
5. **Furhman, J., and F. Azam.** 1980. Bacterioplankton secondary production estimates for coastal waters of British Columbia, Antarctica, and California. Appl. Environ. Microbiol. **39**:1085–1095.
6. **Geiskes, W. W. C., G. W. Kraay, and M. A. Baars.** 1979. Current ^{14}C methods for measuring primary production: gross underestimates in oceanic waters. Neth. J. Sea Res. **13**:58–78.
7. **Hagström, A., U. Larsson, P. Hörstedt, and S. Normark.** 1979. Frequency of dividing cells, a new approach to the determination of bacterial growth rates in aquatic environments. Appl. Environ. Microbiol. **37**:805–812.
8. **Hauxhurst, J. D., T. Kaneko, and R. M. Atlas.** 1981. Characteristics of bacterial communities in the gulf of Alaska, USA. Microb. Ecol. **7**:167–182.
9. **Hornbeck, R. W.** 1975. Numerical methods, p. 16–19. Quantum Publishers, New York.
10. **Hulburt, E. M.** 1963. The diversity of phytoplankton populations in oceanic, coastal and estuarine regions. J. Mar. Res. **21**:81–93.
11. **Kaneko, T., R. M. Atlas, and M. Krichevsky.** 1977. Diversity of bacterial populations in the Beaufort Sea. Nature (London) **270**:596–599.
12. **Karl, D. M.** 1979. Measurement of microbial activity and growth in the ocean by rates of stable ribonucleic acid synthesis. Appl. Environ. Microbiol. **38**:850–860.
13. **Karl, D. M.** 1981. Simultaneous rates of ribonucleic acid and deoxyribonucleic acid synthesis for estimating growth and cell division of aquatic microbial communities. Appl. Environ. Microbiol. **42**:802–810.
14. **Karl, D. M., and P. Bossard.** 1985. Measurement and significance of ATP and adenine nucleotide pool turnover in microbial cells and environmental samples. J. Microbiol. Methods **3**:125–139.
15. **Karl, D. M., and P. Bossard.** 1985. Measurement of microbial nucleic acid synthesis and specific growth rate by $^{32}PO_4$ and [^{3}H]adenine: field comparison. Appl. Environ. Microbiol. **50**:706–709.
16. **Karl, D. M., and C. D. Winn.** 1984. Adenine metabolism and nucleic acid synthesis: applications to microbiological oceanography, p. 197–215. *In* J. E. Hobbie and P. J. L. Williams (ed.), Heterotrophic activity in the sea. Plenum Publishing Corp., New York.
17. **Karl, D. M., C. D. Winn, and D. C. L. Wong.** 1981. RNA synthesis as a measure of microbial growth in aquatic environments. I. Evaluation, verification and optimization of methods. Mar. Biol. (Berlin) **64**:1–12.
18. **Laws, E. A., D. G. Redalje, L. W. Haas, P. K. Bienfang, R. W. Eppley, W. G. Harrison, D. M. Karl, and J. Marra.** 1984. High phytoplankton growth and production rates in oligotrophic Hawaiian coastal waters. Limnol. Oceanogr. **29**:1161–1169.
19. **Novitsky, J. A.** 1983. Heterotrophic activity throughout a vertical profile of seawater and sediment in Halifax Harbor, Canada. Appl. Environ. Microbiol. **45**:1753–1760.
20. **Redalje, D. G., and E. A. Laws.** 1981. A new method for estimating phytoplankton growth rates and carbon biomass. Mar. Biol. (Berlin) **62**:73–79.
21. **Rivkin, R. B., and H. H. Seliger.** 1981. Liquid scintillation counting for ^{14}C uptake of single algal cells isolated from natural samples. Limnol. Oceanogr. **26**:780–785.
22. **Rivkin, R. B., E. Swift, W. H. Biggley, and M. A. Voytek.** 1984. Growth and carbon uptake by natural populations of oceanic dinoflagellates *Pyrocystis noctiluca* and *P. fusiformis*. Deep-Sea Res. **31**:353–367.
23. **Seinfeld, J. H., and L. Lapidus.** 1974. Mathematical methods in chemical engineering, vol. 3. Process modeling, estimation, and identification, p. 289–294. Prentice-Hall, Inc., Englewood Cliffs, N.J.
24. **Sheldon, R. W., and W. H. Sutcliffe, Jr.** 1978. Generation time of 3h for Sargasso Sea microplankton determined by ATP analysis. Limnol. Oceanogr. **23**:1051–1055.
25. **Stahl, D. A., D. J. Lane, G. J. Olsen, and N. R. Pace.** 1984. Analysis of hydrothermal vent-associated symbionts by ribosomal RNA sequences. Science **224**:409–411.
26. **Taguchi, S., and E. A. Laws.** 1985. Application of a single cell isolation technique to studies of carbon assimilation by the subtropical silicoflagellate *Dictyocha perlaevis*. Mar. Ecol. Prog. Ser. **23**:251–255.
27. **Weiler, C. S.** 1980. Population structure and *in situ* division rates of *Ceratium* in oligotrophic waters of the north Pacific central gyre. Limnol. Oceanogr. **25**:610–619.
28. **Weiler, C. S., and S. W. Chisholm.** 1976. Phased cell division in natural populations of marine dinoflagellates from shipboard cultures. J. Exp. Mar. Biol. Ecol. **25**:239–247.

Downloaded from aem.asm.org at Univ of Hawaii at Manoa on March 30, 2010